Towards the Control of Multistability, in a PWM-Driven DC Motor Drive by Short Forcing

Oleksiy Kuznyetsov[1,2]

[1]Department of Electromechanics and Electronics, Hetman Petro Sahaidachnyi National Army Academy, 32 Heroiv Maidanu Str., 79026, Lviv, Ukraine

[2]Institute of Power Engineering and Control Systems, Lviv Polytechnic National University, 12 S. Bandera Str., 79000, Lviv, Ukraine
oleksii.o.kuznietsov@lpnu.ua

Abstract: PWM-driven feedback systems are known for demonstrating the multistable behavior within the stability margins of a nominal operating mode. With the transition of the system to the stable coexisting mode, the ripples of the variables increase and the overall efficiency deteriorates; therefore, it is an undesired behavior. We study the possibility of controlling multistability on the model of a chopper-fed DC drive. The proposed control takes the form of short forcing, temporarily moving the margins between the basins of attraction of the coexisting modes and thus driving the system to the nominal mode of operation. We also propose a universal control strategy, combining different types of short forcing, that are applied in a repeated manner with different settings. The latter control strategy overcomes unpredictability of the system's behavior caused by the fractal basin boundaries, and also, by external disturbances or noise.

Keywords: DC drive; multistability; basin of attraction; control of multistability

1 Introduction

Pulse width modulation (PWM) is a common solution for high-efficiency voltage regulation. In technical systems, it is implemented with the use of different topologies of power converters [1]. Accompanied with a microprocessor or a microcontroller unit [2] [3], it provides the possibility to implement complicated control strategies [4], in particular, for electric drives and servo systems; these are fuzzy-logic-based control [5], neuro-fuzzy-based control [6], model predictive control [7], reinforcement-learning-based control [8], *etc.*

The synthesis of the control strategy and parameter tuning, besides the task of providing the desirable static and dynamic indices, has to deal with the stability issues. With the assumption that the system's behavior is approximated as a linear system, we obtain the advantage of a well-developed synthesis and stability theory

for linear systems [2]. Alternatively, optimization algorithms are applied to tune classical linear controllers [9] or nonlinear controllers are synthesized to ensure robustness of the system [10].

However, with the inclusion of switching power converters, the system obtains the special type of nonlinearity—the switching one. Thus, if a simple electric circuit is combined of a resistor, a capacitor, and an inductor it is mathematically well represented by a simple linear time-invariant dynamical system. However, if the considered circuit is fed by a PWM-driven converter with a voltage or current feedback, the system becomes piecewise-linear leading to different nonlinear phenomena [11].

These phenomena have obtained a well-elaborated theory and were experimentally observed [11]. Electric drive systems fed from power electronic converters inhere their features [12]. In the current work, we focus on one of these features, *multistability*—the coexistence of several stable modes of operation for the same set of parameters. Multistability itself is a general feature of many physical systems of different nature and is observed both theoretically and experimentally [13] [14]. Each of the coexisting stable modes has its own *basin of attraction*—the set of initial states from which the trajectory of the system is attracted to the particular mode. Under noise or external disturbances, the transition between the coexisting states can occur—what is known as *tipping* [15] [16]. Those phenomena corresponding to multistability are also observed in switching power converters [17-19].

In PWM-controlled systems, the nominal operating mode is characterized by the lowest ripples of the system variables; therefore, the operation in any other coexisting mode is characterized by lower efficiency and should be avoided. It is worth noting that synthesis and tuning techniques take into account the nominal operating mode, neglecting the possible coexisting modes; however, they can have harmful effects on the system's behavior [20] [21].

What is utilized as a case study for our current work, a chopper-fed DC drive (Fig. 1a) under the parameters as given in Appendix, is known for demonstrating multistability [22] (see also [23]). Previously, we have depicted phenomena related to tipping in the considered system [24] [25]. What is sufficient for our study, it is demonstrated in [24] that the nominal mode is the most robust-to-noise among the coexisting ones for several sets of parameters.

Controlling multistability itself is of interest to scientific community [26]. The solutions can be classified into two categories: (i) the system is driven to a desired regime by some perturbation [27-29] and (ii) the undesired regime is annihilated under implementing some control [30-35].

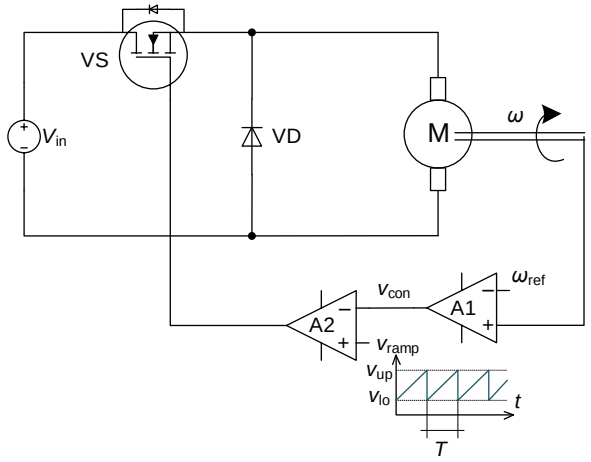

Figure 1
Circuit diagram of a chopper-fed DC drive, after [12]

It is obvious that the best solution is the second one ensuring the monostability operation of the system. However, several control techniques require the knowledge of the system dynamics, such as the linear augmentation technique [32], while others are based on the use of periodic modulation [30] [31] and are simple in implementation and tuning. On the other hand, adding additional control loops is in many cases undesirable as far as it complicates the tuning of the controller to achieve the control tasks (*e.g.* speed of operation, overshoot, *etc.*). In contradiction to those techniques, in the current work, we elaborate the first solution as being simpler for implementation. In general, the perturbation can be implemented in the form of constant periodic action [28], temporal feedback [29], or short pulses [27].

In a PWM-driven system, the perturbation can be applied in the form of slight changes of the switching function. The idea has been theoretically proven for extending the stability margins of the nominal regime [36] [37] (however, it requires constant control).

In the current work, our idea is that the same short disturbing action as in [37] has been developed specifically for the switching power converters (but with the different purpose and implemented as a constant action) slightly varies the margins of the basins of attraction of the coexisting modes. Hence, being shortly applied, as it has been proposed in [27] for a laser system, the control in the form of short perturbations can drive system to the nominal regime. Thus, the proposed control strategy uses short forcing only to force the system to return to the desired nominal mode of operation if a multistable system tips to the undesired mode and is only applied if the coexisting mode is detected. Therefore, the objective of the study is to obtain an advantage of the simple for implementation controller that can guarantee the nominal operation of the system.

2 Mathematical Model of a DC Drive

2.1 Mathematical Model in Continuous Time

The system under analysis is a permanent magnet DC motor fed from a chopper in the form of buck converter with the speed feedback loop and PWM-2 control (Fig. 1a).

The state of the switch VS is dictated by the relation between the values of a control signal v_{con} and a carrier (ramp) signal v_{ramp}. Thus, if $v_{\text{con}} < v_{\text{ramp}}$, the switch is on, and the system is depicted by the equation

$$\frac{d}{dt}\begin{bmatrix}\omega(t)\\ i(t)\end{bmatrix} = \begin{bmatrix}-\frac{B}{J} & \frac{K_T}{J}\\ -\frac{K_E}{L} & -\frac{R}{L}\end{bmatrix}\begin{bmatrix}\omega(t)\\ i(t)\end{bmatrix} + \begin{bmatrix}-\frac{T_L}{J}\\ \frac{V_{\text{in}}}{L}\end{bmatrix} \tag{1a}$$

while if $v_{\text{con}} \geq v_{\text{ramp}}$, the switch is off, and

$$\frac{d}{dt}\begin{bmatrix}\omega(t)\\ i(t)\end{bmatrix} = \begin{bmatrix}-\frac{B}{J} & \frac{K_T}{J}\\ -\frac{K_E}{L} & -\frac{R}{L}\end{bmatrix}\begin{bmatrix}\omega(t)\\ i(t)\end{bmatrix} + \begin{bmatrix}-\frac{T_L}{J}\\ 0\end{bmatrix} \tag{1b}$$

where the notation is explained in the Appendix. Given

$$\mathbf{A} = \begin{bmatrix}-B/J & K_T/J\\ -K_E/L & -R/L\end{bmatrix},\ \mathbf{x} = \begin{bmatrix}\omega(t)\\ i(t)\end{bmatrix},\ \mathbf{E}_{\text{off}} = \begin{bmatrix}-T_L/J\\ 0\end{bmatrix},\ \mathbf{E}_{\text{on}} = \begin{bmatrix}-T_L/J\\ V_{\text{in}}/L\end{bmatrix}$$

the system is represented by the state-space equation dependent on the state of the switch VS:

$$\dot{\mathbf{x}} = \mathbf{A}\mathbf{x} + \mathbf{E}_k \tag{2}$$

where $\mathbf{E}_k$, $k = \{\text{on}, \text{off}\}$ is the product $\mathbf{Bu}$ from the standard state-space representation, is the subscript representing the state of the switch VS.

For the sawtooth carrier signal with the ramp period T:

$$v_{\text{ramp}}(t) = v_{\text{lo}} + \left(v_{\text{up}} - v_{\text{lo}}\right)\left(\frac{t}{T} \bmod 1\right) \tag{3}$$

where v_{lo} and v_{up} are lower and upper levels of the sawtooth signal (Fig. 1). With a proportional speed controller, the control signal v_{con} is:

$$v_{\text{con}}(t) = g(\omega(t) - \omega_{\text{ref}}) \tag{4}$$

where g is a feedback gain, $\omega(t)$ is instantaneous speed, and ω_{ref} is the reference speed.

2.2 Derivation of Discrete-Time Mapping

For the purposes of analyzing the periodic steady state of the system, and since the behavior of the system is governed by the clock cycle T, it is natural to obtain a discrete-time model in the form of "stroboscopic" mapping $\mathbf{x}_{n+1} = P(\mathbf{x}_n)$ synchronized with the period T (as it has been explained in [11]), where $\mathbf{x}_n = \mathbf{x}(t_0)$, and $\mathbf{x}_{n+1} = \mathbf{x}(t_0 + T)$, where the evolution of the system between periodic instances is governed by the continuous-time model, here, (1-4). The model (1-4) was implemented in the Matlab environment utilizing the `ode45` solver with the built-in event detection.

3 Periodic Steady State of the System

With the derived discrete-time stroboscopic mapping, an arbitrary nT-periodic steady state is reduced to a period-n mode of the stroboscopic map. In particular, the nominal period-1 mode of the stroboscopic map (nT-periodic mode of the system, its period is equal to the clock cycle T) corresponds to a fixed point of a stroboscopic map, $2T$-periodic, to period-2 mode, *etc*.

The previous publications [22] [23] have demonstrated the coexistence of several stable regimes for the same parameters of the considered system (the parameters are given in the Appendix). The time-domain and state-space representation of the coexisting modes are demonstrated in Fig. 2 and Fig. 3, respectively. In Fig. 2 and Fig. 3, the corresponding discrete-time cycles (sampling of the continuous-time model) are marked with circles.

Comparing the three coexisting stable modes (Figs. 2 and 3), it is obvious that higher-periodic modes are situated in the same area of the state space, however, they are characterized by the higher ripples of the state variables. Therefore, from the practitioner's point of view, they correspond to undesirable lower-efficiency modes and should be avoided. On the other hand, the ripples can be measured and used to evaluate whether the system operates in its nominal mode or not.

Previously [23], we have analyzed the evolution of the coexisting regimes as the feedback gain g varies by means of the bifurcation diagrams. Afterwards, we have analyzed the behavior of the system for several gain values corresponding to several coexistence scenarios (those depicted in Fig. 4, period-1 and chaotic mode for g = 1.195, period-1, -3 and -4 for g = 2, and period-1 and period-6, for g = 2.2) [24]. What was also observed in [24] is that the nominal period-1 regime for all analyzed cases $g = \{1.195; 2; 2.2\}$ is the most robust to noise and external disturbances. Below, we also utilize the studies of the basins of attraction of the coexisting periodic modes to understand that kind of behavior of the regimes.

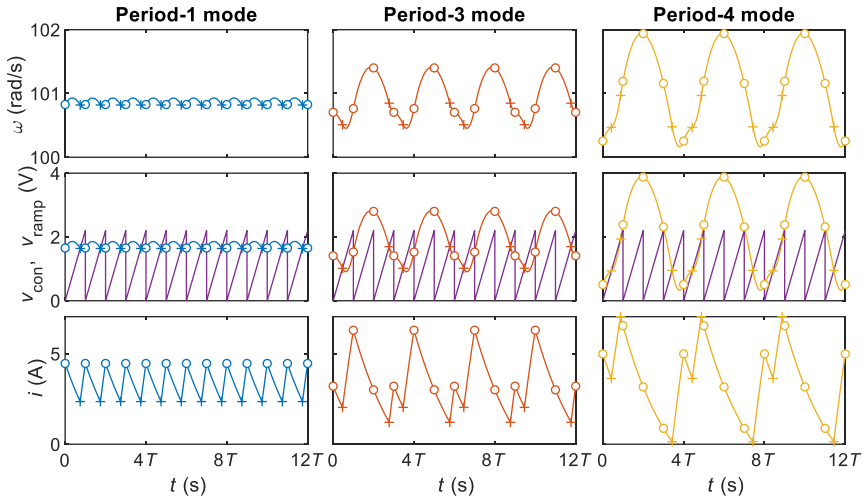

Figure 2
Trajectories of the coexisting period-1, -3 and -4 modes in the time domain, after [23]

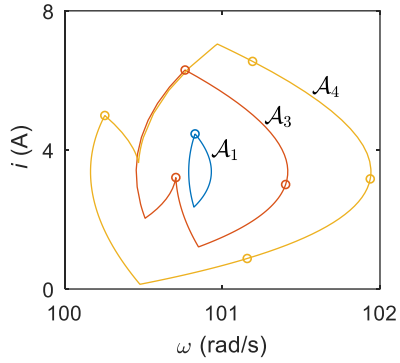

Figure 3
Trajectories $\mathcal{A}_i$ of the coexisting period-i modes, $i = \{1; 3; 4\}$, in the state-space, after [23]

4 Basins of Attraction of the Coexisting Regimes

Proceeding to studying multistability in the considered system, we analyze the basins of attraction for several values of gain g (corresponding to the values denoted in Fig. 3). The basins of attraction are depicted in Fig. 5 for the grid 500×500 of initial conditions, where $\mathcal{B}_i$ stands for the basin of attraction of the period-i mode (and χ is used for chaotic mode).

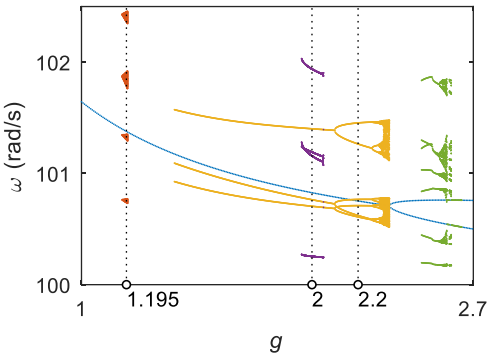

Figure 4
Several cases of coexisting stable modes at the bifurcation diagram of the speed ω taking feedback gain g as a parameter

The general feature is that for all analyzed cases in Fig. 4, we observe the complex interwoven structure of the basins, resulting in the practical unpredictability of the behavior. However, we summarize the basins have one thing common—the basins of the nominal period-1 mode near the point of its steady-state operation has the largest distance to the basin margin. That is demonstrated in Fig. 5 (the blow-up of the marked area in Fig. 4) for the case $g = 2$, the same can be observed in other cases. The basins of the coexisting states can be characterized by the commensurate distance to the margin (as $\mathcal{B}_3$ for $g = 2$ and $\mathcal{B}_6$ for $g = 2.2$) or lower (as $\mathcal{B}_\chi$ for $g = 1.195$ and $\mathcal{B}_4$ for $g = 2$). That determines the robustness of a mode to external action. In Fig. 5, red circle stands for period-1 mode, blue for period-3, and yellow for period-4.

5 Control of Multistability by Short Forcing

Between the periodic instances, the switch changes its state if the switching function $h(\mathbf{x}, t) = 0$ is satisfied. For the analyzed system, as it has been explained in the Modelling Section 2.1, $h(\mathbf{x}, t) = v_{\text{con}}(t) - v_{\text{ramp}}(t) = 0$ and therefore it is defined after (3) and (4) as follows:

$$h(\mathbf{x}, t) = g(\omega(t) - \omega_{\text{ref}}) - \left(v_{\text{lo}} + \left(v_{\text{up}} - v_{\text{lo}}\right)t^*\right) \tag{5}$$

where for ease of representation we use $t^* = t \bmod T$ as the time from the beginning of the examined period. The block diagram of the PWM signal generation corresponding to (5) is depicted in Fig. 7.

The three considered control strategies rely on slightly changing the switching function (5). The same idea is applied in [36] [37] with the other purpose of extending the stability margins of the nominal regime by stabilizing the period-1 mode becoming unstable.

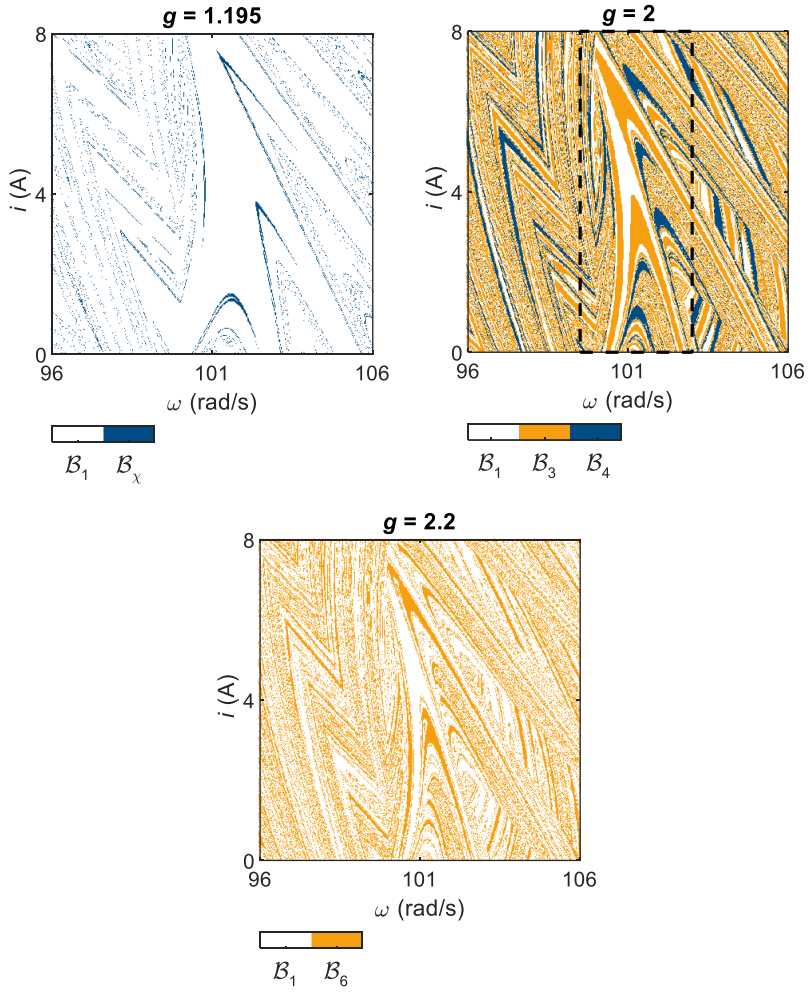

Figure 5

Basins of attraction $\mathcal{B}_i$ of coexisting stable states for several values of gain g corresponding to Fig. 4

Respectively, in our work, we consider that slight changes of the switching function slightly move the margins of the basins of the coexisting regimes, therefore, it can result in the tipping between the coexisting modes. As to our knowledge, the technique has never been applied to control the tipping between the coexisting modes. Below, we propose several strategies of modifying the switching function and analyze the system's behavior under those actions.

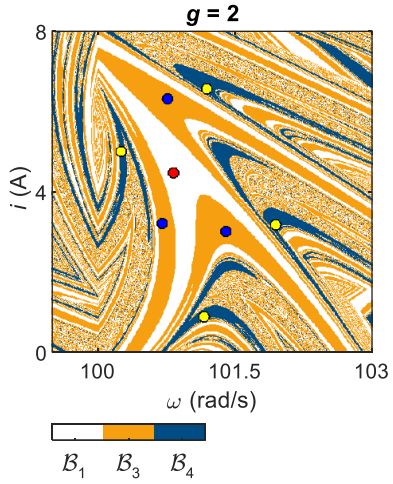

Figure 6
Blow-up of the marked region of the basins of attraction in Fig. 5 with the corresponding sampled periodic modes

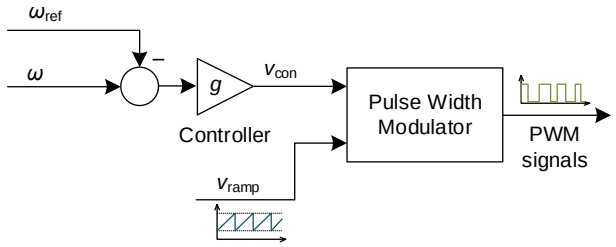

Figure 7
Block diagram of the PWM signals generation corresponding to the switching function $h(\mathbf{x}, t)$, (5)

In Figs. 9-11, the corresponding control strategies are applied within the shaded area, refer to the captions for explanation. In the figures below, circles stand for samples (discrete-time model), while crosses for switching.

5.1 Strategy 1: Utilizing an Additional Sinusoidal Perturbation of the Reference Signal

The first strategy is based on slight sinusoidal changes of the reference signal ω_{ref}:

$$h_1(\mathbf{x}, t) = g\left(\omega(t) - \omega_{\text{ref}}\left(1 - a \sin\frac{2\pi t^*}{T}\right)\right) - \left(v_{\text{lo}} + \left(v_{\text{up}} - v_{\text{lo}}\right)t^*\right) \tag{6}$$

where a is an adjustment coefficient for the strategy (6) as well as for those discussed below. For the purposes of the current study, its value is not under discussion, as far as we aim to analyze the general behavior under the proposed

control. In the study, the value is taken as $a = 10^{-3}$. The PWM signal generation block diagram corresponding to the strategy (6) is demonstrated in Fig. 8a (the control is enabled if the function $k_1(t)$ is ON).

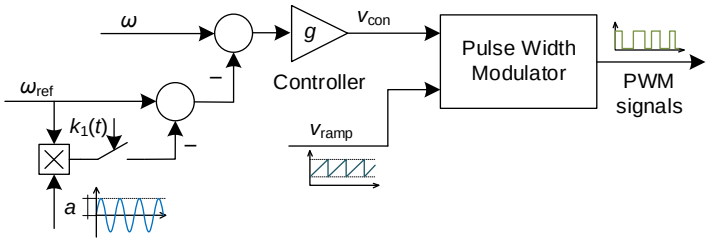

(a)

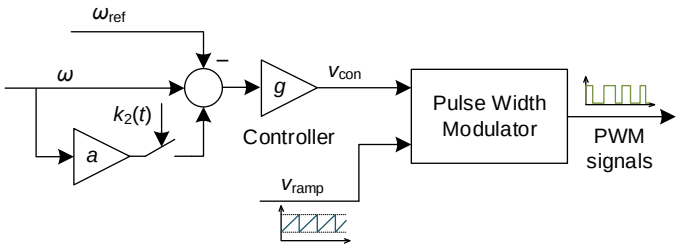

(b)

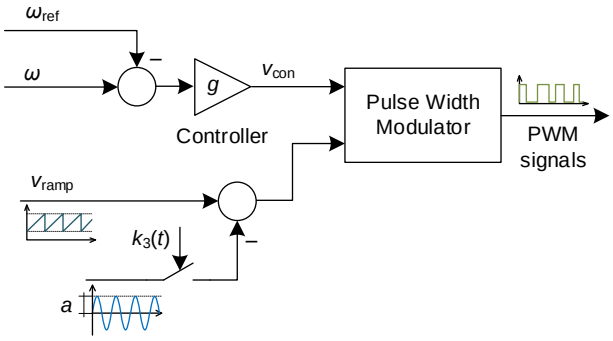

(c)

Figure 8

Block diagrams of the PWM signals generation corresponding to the switching functions $h_1(\mathbf{x}, t)$, equation (6) (a), $h_2(\mathbf{x}, t)$, equation (7) (b), and $h_3(\mathbf{x}, t)$, equation (8) (c)

5.2 Strategy 2: Adding a Signal Proportional to a State Variable

The second possible control strategy (Fig. 8b, enabled by $k_2(t)$) corresponds to the addition of the signal proportional to $\omega(t)$:

$$h_2(\mathbf{x},t) = g\big((1+a)\omega(t) - \omega_{\mathrm{ref}}\big) - \big(v_{\mathrm{lo}} + \big(v_{\mathrm{up}} - v_{\mathrm{lo}}\big)t^*\big) \tag{7}$$

5.3 Strategy 3: Utilizing an Additional Sinusoidal Perturbation of the Carrier Signal

And the third strategy (Fig. 8c, enabled by $k_3(t)$) utilizes sinusoidal perturbation applied to the carrier ramp signal:

$$h_3(\mathbf{x},t) = g(\omega(t) - \omega_{\mathrm{ref}}) - \left(v_{\mathrm{lo}} + \big(v_{\mathrm{up}} - v_{\mathrm{lo}}\big)t^* - a\sin\frac{2\pi t^*}{T}\right) \tag{8}$$

5.4 Discussion and Proposal of a Combined Control Strategy

Let us analyze the observations depicted in Figs. 7-9, where the results of applying different control strategies to the system operating in the coexisting modes are demonstrated.

First, we should keep in mind that the proposed control strategies are related to slight changes of basin margins; therefore, they cause controlled tipping from one mode to another one. However, some other perturbations being applied simultaneously (*e.g.*, noise), can cause changes to the direction of tipping.

Second, in the proposed solution, there is no such control strategy that, being applied to the system, causes tipping *exactly* to the desired mode; even if simulation demonstrates that behavior for some parameter set, there is no guarantee the same occurs under real-world conditions with inevitable noise and parameter variation (therefore, due to the complex structure of basin boundaries, see Fig. 5, the tipping in a real application becomes absolutely unpredictable).

Third, for the selected value of a, there is no transition from the nominal period-1 regime to some other; however, there is no guarantee that it will not occur under real-world conditions.

With the above mentioned considerations, our proposal is to apply a combined control strategy including the following. The control should be applied if the system operates in the undesired coexisting stable mode in the steady state; if the control action results in tipping to the undesired mode, the control should be applied again. As it has already been mentioned, the detection of the undesired mode can be applied in the form of detecting the increased ripples of variables.

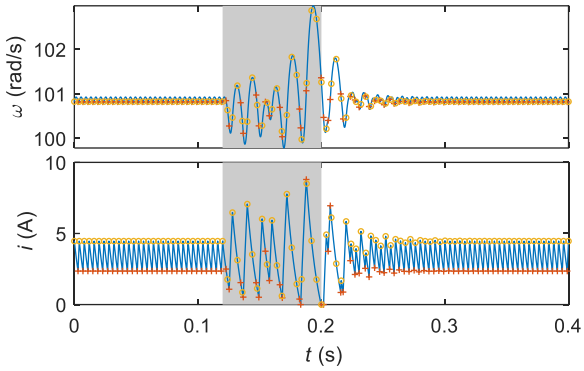

(a) from period-1 mode

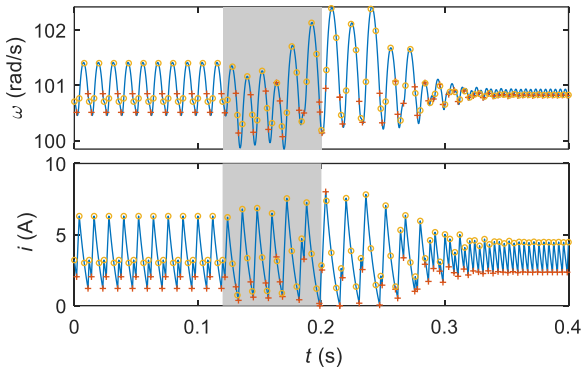

(b) from period-3 mode

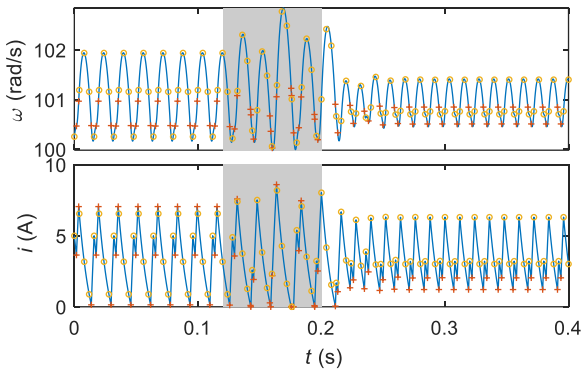

(c) from period-4 mode

Figure 9
Transitions from the coexisting modes corresponding to implemented Strategy 1—for utilizing an additional sinusoidal perturbation of the reference signal

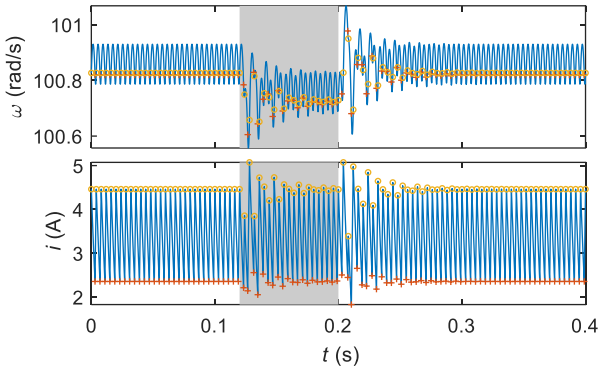

(a) from period-1 mode

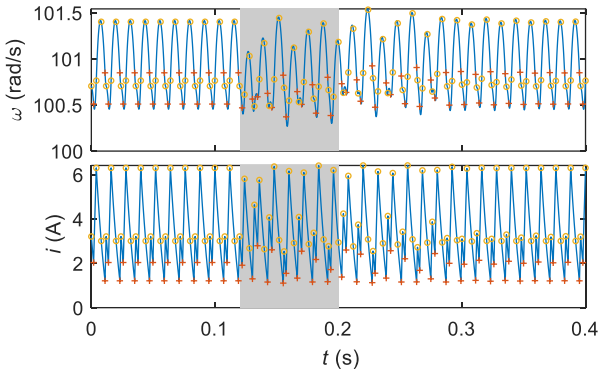

(b) from period-3 mode

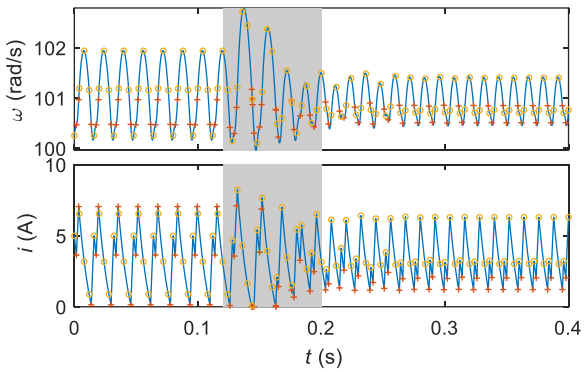

(c) from period-4 mode

Figure 10

Transitions from the coexisting modes corresponding to the implemented Strategy 2—for adding a signal proportional to a state variable

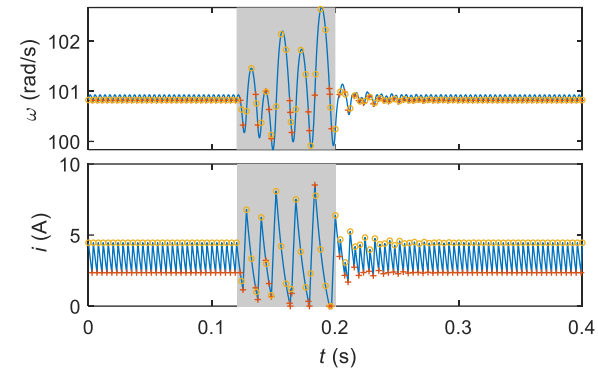

(a) from period-1 mode

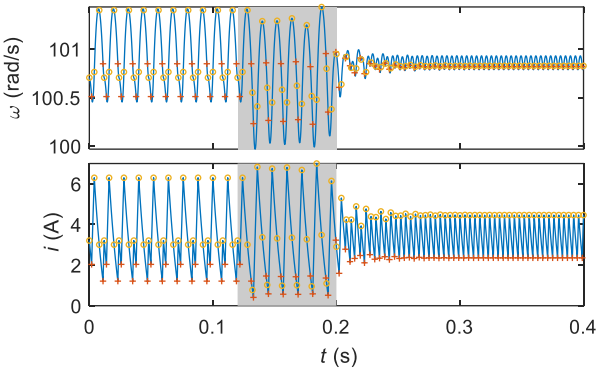

(b) from period-3 mode

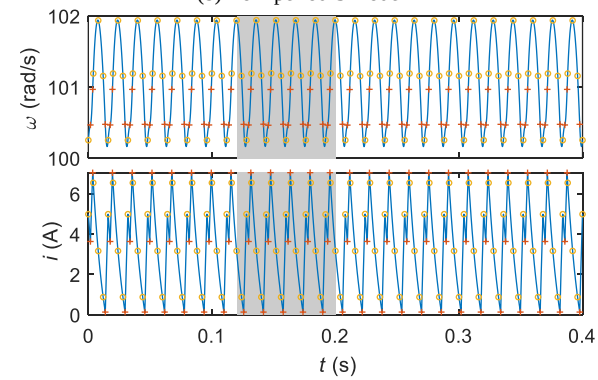

(c) from period-4 mode

Figure 11

Transitions from the coexisting modes corresponding to the implemented Strategy 3—for utilizing an additional sinusoidal perturbation of the carrier signal

The next consideration is that we should apply different control strategies alternately to avoid the situation demonstrated in Fig. 11c, where applying the

control action causes no transition to another mode (and even no noticeable transients).

Now, let us summarize the observations and formulate the requirements for the combined control. Thus, there is no universal control strategy that inevitably drives the system to the nominal period-1 mode (in general, we should assume that no tuning of the control strategies (6)–(8), selecting the modulation coefficient a and a forcing duration t, guarantee to obtain a universal controller). Then, the universal combined control strategy should contain several different forcing types repeated cyclically until the nominal mode is achieved. The example algorithm is depicted by the flowchart in Fig. 12. It corresponds to the application of the three depicted control strategies (6-8) repeatedly, that case is used for the simulations in Fig. 13. However, it is worth noting that in general, the base of forcing types can be widened by using different coefficient a and t values.

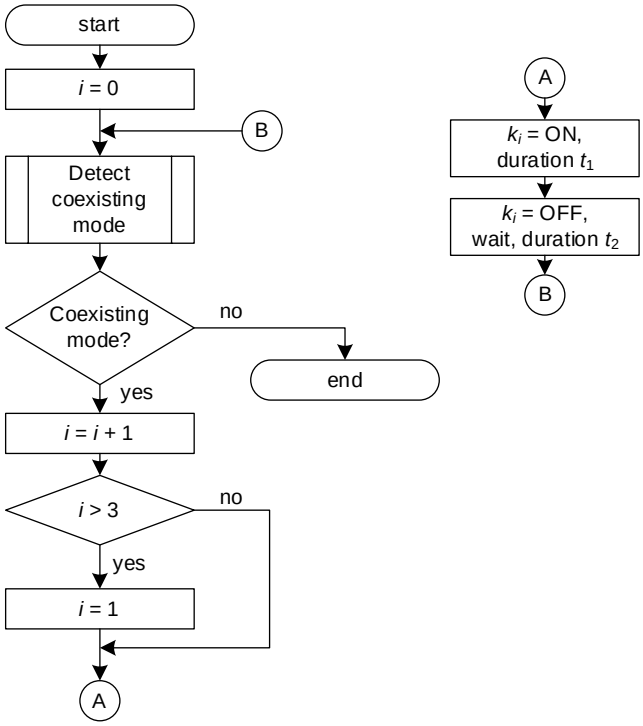

Figure 12
Flowchart of the concept of a combined control strategy

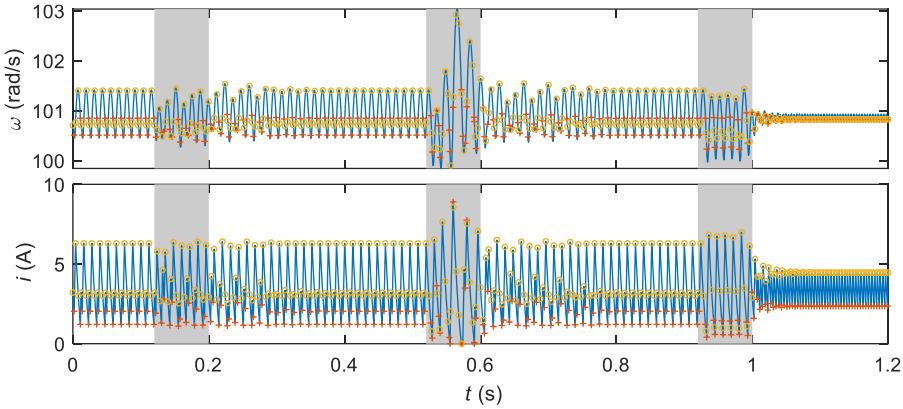

(a) from period-3 mode

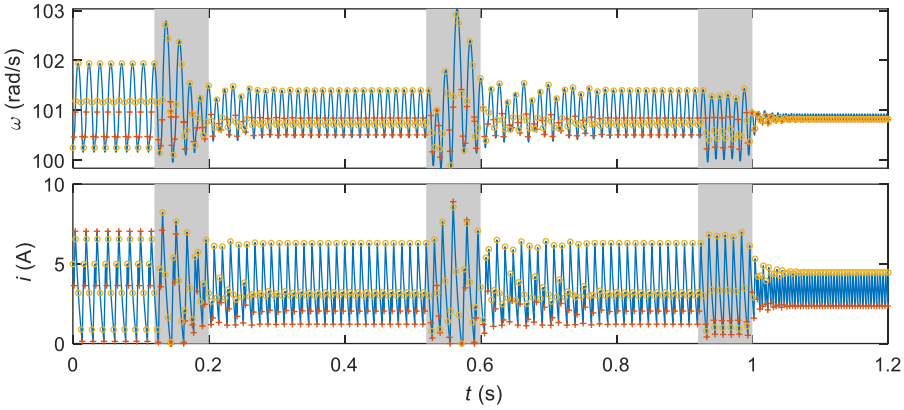

(b) from period-4 mode

Figure 13
Example of application of a combined control strategy (Strategy 2 → Strategy 1 → Strategy 3)

Conclusions

As it is known, in a PWM-controlled feedback system, different nonlinear behaviors can be observed, including multistability—the coexistence of several stable periodic modes for the same set of parameters; particularly, within the stability margins of the nominal operating mode it is an undesired behavior. In a coexisting mode, the overall system's efficiency deteriorates and that determines the requirement to have the possibility of controlling multistability, *i.e.* to guarantee the nominal operating mode.

In the example of a chopper-fed DC drive, we study the possibility of controlling multistability by short forcing. That is applied in the form of short, slight changes of the PWM switching function, slightly moving the margins between the basins of the coexisting mode resulting in a tipping between the coexisting modes. Several control strategies could be proposed with different disturbing actions applied.

To obtain a universal control algorithm, we propose a control strategy that combines different types of short forcings, that are applied in a repeated manner. That also guarantees that the system is driven, after several iterations, to its nominal mode even if it is subjected to any external disturbances (*e.g.* noise) thus overcoming the unpredictability of the system's behavior caused by the fractal boundaries of the basin of attraction.

Appendix: Parameters of the DC Drive [22]

Ramp voltage: Lower level $v_{\mathrm{lo}} = 0$ V, upper level $v_{\mathrm{up}} = 2.2$ V, period $T = 4$ ms

DC motor and load: Armature resistance $R = 3.5\ \Omega$, armature inductance $L = 36$ mH, back-EMF constant $K_E = 0.1356$ V·s, torque constant $K_T = 0.1324$ N·m/A, viscous damping $B = 0.000564$ N·m·s, load inertia $J = 0.000971$ N·m·s^2, load torque $T_{\mathrm{L}} = 0.39$ N·m

Control system: Input voltage $V_{\mathrm{in}} = 100$ V, feedback gain $g = 2$, reference speed $\omega_{\mathrm{ref}} = 100$ rad/s

References

[1] B. K. Bose, *Power Electronics and Motor Drive Advances and Trends*. MA, Burlington: Elsevier, 2006

[2] C. A. Iordache, M. Bodea, "Analysis and design of a high efficiency current mode buck converter with I^{2}C controlled output voltage," *Roman. J. Inform. Sci. Technol.*, Vol. 23, No. 2, pp. 188-203, 2020

[3] T. S. Kumar and R. N. Banavar, "Observer based control of a brushed DC motor at very low speeds over controller area network: An application in astronomical telescopes," in *2017 11th Asian Control Conf. (ASCC)*, Dec. 2017, pp. 1449-1453, doi: 10.1109/ASCC.2017.8287386

[4] D. A. Barkas, G. C. Ioannidis, C. S. Psomopoulos, S. D. Kaminaris, and G. A. Vokas, "Brushed DC Motor Drives for Industrial and Automobile Applications with Emphasis on Control Techniques: A Comprehensive Review," *Electronics*, Vol. 9, No. 6, Art. No. 887, May 2020, doi: 10.3390/electronics9060887

[5] R.-E. Precup *et al.*, "Generic two-degree-of-freedom linear and fuzzy controllers for integral processes," *J. Franklin Inst.*, Vol. 346, No. 10, pp. 980-1003, 2009, doi: 10.1016/j.jfranklin.2009.03.006

[6] Y. Paranchuk, P. Evdokimov, and O. Kuznyetsov, "Electromechanical positioning system with a neuro-fuzzy corrector," *Przegl. Elektrotechn.*, Vol. 96, No. 9, 2020, doi: 10.15199/48.2020.09.11

[7] A. Reda, A. Bouzid, J. Vásárhelyi, "Model predictive control for automated vehicle steering," *Acta Polytechn. Hungar.*, Vol. 17, No. 7, pp. 163-182, 2020, doi: 10.12700/APH.17.7.2020.7.9

[8] I. A. Zamfirache, R.-E. Precup, R.-C. Roman, E. M. Petriu, "Reinforcement Learning-based control using Q-learning and gravitational search algorithm with experimental validation on a nonlinear servo system," *Inform Sci.*, Vol. 583, pp. 99-120, 2022, doi: 10.1016/j.ins.2021.10.070

[9] R.-C. Roman *et al.*, "Iterative Feedback Tuning Algorithm for Tower Crane Systems," *Procedia Comp. Sci.*, Vol. 199, pp. 157-165, 2021, doi: 10.1016/j.procs.2022.01.020

[10] R.-E. Precup, S. Preitl, "PI-Fuzzy controllers for integral plants to ensure robust stability," *Inform. Sci.*, Vol. 177, No. 20, pp. 4410-4429, 2007, doi: 10.1016/j.ins.2007.05.005

[11] S. Banerjee and G. C. Verghese, Eds., *Nonlinear Phenomena in Power Electronics: Bifurcations, Chaos, Control, and Applications*. Wiley-IEEE Press, 2001

[12] K. T. Chau and W. Zheng, *Chaos in Electric Drive Systems: Analysis, Control and Application*. Wiley-IEEE Press, mar 2011

[13] U. Feudel, "Complex dynamics in multistable systems," *Int. J. Bifurc. Chaos*, Vol. 18, No. 6, pp. 1607-1626, 2008, doi: 10.1142/ S0218127408021233

[14] A. N. Pisarchik, A. E. Hramov, *Multistability in Physical and Living Systems: Characterization and Applications*. Springer, 2022

[15] U. Feudel, A. N. Pisarchik, and K. Showalter, "Multistability and tipping: From mathematics and physics to climate and brain—Minireview and preface to the focus issue," *Chaos*, Vol. 28, No. 3, Art. No. 033501, mar 2018, doi: 10.1063/1.5027718

[16] G. Ambika, J. Kurths, "Tipping in complex systems: theory, methods and applications," *Eur. Phys. J. Spec. Top*., Vol. 230, pp. 3177-3179, 2021, doi: 10.1140/epjs/s11734-021-00281-z

[17] Z. T. Zhusubaliyev and E. Mosekilde, "Multistability and hidden attractors in a multilevel DC/DC converter," *Math. Computers Simulation*, Vol. 109, pp. 32-45, 2015, doi: 10.1016/j.matcom.2014.08.001

[18] A. el Aroudi, J. Huang, M. S. Al-Numay, and Z. Li, "On the Coexistence of Multiple Limit Cycles in H-Bridge Wireless Power Transfer Systems With Zero Current Switching Control," *IEEE Trans. Circ. Syst. I: Reg. Papers*, Vol. 67, No. 5, pp. 1729-1739, May 2020, doi: 10.1109/TCSI.2019.2960575

[19] L. Benadero, E. Ponce, A. el Aroudi, and L. Martinez-Salamero, "Analysis of coexisting solutions and control of their bifurcations in a parallel LC resonant inverter," in *Proc. IEEE Int. Symp. Circ. Syst.*, May 2017, pp. 1-4, doi: 10.1109/ISCAS.2017.8050512

[20] M. A. Kiseleva, N. V. Kuznetsov, and G. A. Leonov, "Hidden attractors in electromechanical systems with and without equilibria," *IFAC-*

PapersOnLine, Vol. 49, No. 14, pp. 51-55, Jan. 2016, doi: 10.1016/J.IFACOL.2016.07.975

[21] H. Kim, S. H. Lee, J. Davidsen, and S. W. Son, "Multistability and variations in basin of attraction in power-grid systems," *New J. Phys.*, Vol. 20, No. 11, p. 113006, 2018, doi: 10.1088/1367-2630/aae8eb

[22] N. Okafor, "Analysis and Control of Nonlinear Phenomena in Electrical Drives," Ph.D. dissertation, Newcastle University, Newcastle, UK, 2012

[23] O. O. Kuznyetsov, "Calculation of stable and unstable periodic orbits in a chopper-fed DC drive," *Math. Modeling Comput.*, Vol. 8, No. 1, pp. 43-57, 2021, doi: 10.23939/mmc2021.01.043

[24] O. Kuznyetsov and Y. Paranchuk, "Remarks on the behavior of a multistable DC drive in the presence of noise," *2021 IEEE 12th Int. Conf. Electron. Inf. Technol. (ELIT)*, Lviv, Ukraine, 2021, pp. 175-180, doi: 10.1109/ELIT53502.2021.9501090

[25] O. Kuznyetsov and Y. Paranchuk, "Phenomena related to noise-induced and disturbance-induced tipping in a multistable DC drive," *IEEE EUROCON 2021 - 19th Int. Conf. Smart Technol.*, Lviv, Ukraine, 2021, pp. 408-413, doi: 10.1109/EUROCON52738.2021.9535584

[26] A. N. Pisarchik and U. Feudel, "Control of multistability," *Phys. Rep.*, Vol. 540, No. 4, North-Holland, pp. 167-218, Jul. 30, 2014, doi: 10.1016/j.physrep.2014.02.007

[27] B. K. Goswami and A. N. Pisarchik, "Controlling multistability by small periodic perturbation," *Int. J. Bifurc. Chaos*, Vol. 18, No. 06, pp. 1645-1673, Jun. 2008, doi: 10.1142/S0218127408021257

[28] F. Hegedűs, W. Lauterborn, U. Parlitz, and R. Mettin, "Non-feedback technique to directly control multistability in nonlinear oscillators by dual-frequency driving," *Nonlin. Dyn.*, Vol. 94, No. 1, 2018, pp. 273-293, doi: 10.1007/s11071-018-4358-z

[29] K. Yadav, A. Prasad, and M. D. Shrimali, "Control of coexisting attractors via temporal feedback," Phys. Lett., Sect. A: Gen., Atomic Solid State Phys., Vol. 382, pp. 2127-2132, aug 2018, doi: 10.1016/ j.physleta.2018.05.041

[30] R. Sevilla-Escoboza, A. N. Pisarchik, R. Jaimes-Reátegui, and G. Huerta-Cuellar, "Selective monostability in multi-stable systems," *Proc. Royal Soc. A: Math., Phys. Eng. Sci.*, 2015, doi: 10.1098/rspa.2015.0005

[31] R. Sevilla-Escoboza et al., "Error-feedback control of multistability," *J. Franklin Inst.*, Vol. 354, No. 16, pp. 7346-7358, Nov. 2017, doi: 10.1016/j.jfranklin.2017.08.052

[32] Z. T. Njitacke et al., "Control of Coexisting Attractors with Preselection of the Survived Attractor in Multistable Chua's System: A Case Study," *Complexity*, Vol. 2020, pp. 1-16, Sep. 2020, doi: 10.1155/2020/5191085

[33] A. el Aroudi, L. Benadero, E. Ponce, C. Olalla, F. Torres, and L. Martinez-Salamero, "Suppression of Undesired Attractors in a Self-Oscillating H-Bridge Parallel Resonant Converters under Zero Current Switching Control," *IEEE Trans. Circ. Syst. II: Expr. Briefs*, Vol. 66, No. 4, pp. 692-696, Apr. 2019, doi: 10.1109/TCSII.2018.2880139

[34] Z. Zhang, J. Páez Chávez, J. Sieber, and Y. Liu, "Controlling grazing-induced multistability in a piecewise-smooth impacting system via the time-delayed feedback control," *Nonlin. Dyn.*, May 2021, doi: 10.1007/s11071-021-06511-2

[35] J. A. Taborda and F. Angulo, "Computing and controlling basins of attraction in multistability scenarios," *Math. Probl. Eng.*, Vol. 2015, pp. 1-13, 2015, doi: 10.1155/2015/313154

[36] D. Giaouris, A. Elbkosh, S. Banerjee, B. Zahawi and V. Pickert, "Control of switching circuits using complete-cycle solution matrices," *2006 IEEE Int. Conf. Ind. Technol.*, 2006, pp. 1960-1965, doi: 10.1109/ICIT.2006.372582

[37] D. Giaouris, S. Banerjee, B. Zahawi and V. Pickert, "Control of Fast Scale Bifurcations in Power-Factor Correction Converters," in *IEEE Trans. Circ. Syst. II: Expr. Briefs*, Vol. 54, No. 9, pp. 805-809, Sept. 2007, doi: 10.1109/TCSII.2007.900350